International Journal of Advanced Science and Technology
Vol.136 (2020), pp.1-10
http://dx.doi.org/10.33832/ijast.2020.136.01

ELECTROMAGNETIC INVESTIGATION OF CYLINDRICAL PHOTONIC CRYSTAL WAVEGUIDES WITH HIGH-INDEX CORES

Jeong Kim[1*]

[1]*Department of Electric, Electronic and Communication Engineering Education, Chungnam National University, Daejeon 34134, South Korea*
[1]jikimi@cnu.ac.kr

***Abstract*— Cylindrical photonic crystal waveguides (CPCWs) with high-index cores are first proposed and analyzed by the accurate full-vector finite difference method and finite-difference time-domain approach. The high-index core can be realized by inserting materials with higher refractive index values than normal pure-silica glass, such as carbon dioxide, liquefied petroleum gas (LPG), and nitrous oxide, into the CPCW. It is generally observed that the high refractive index variation is not linearly changing with the normalized propagation constant. More significant discontinuities in field distributions are also noticed at dielectric boundaries for the CPCW with a lower refractive index core, compared to the CPCW with a higher-index core, which reasonably means that electromagnetic energy is more tightly confined for the CPCW design with the higher-index core.**

***Keywords*— Photonic band-gap, Cylindrical photonic crystal waveguides, Optical components, High-index materials**

1. INTRODUCTION

Photonic crystal structures have gained considerable attention from researchers, who have found innovative applications as in light-emitting diodes, lasers, nonlinear devices, optical fibers, and photovoltaic cells as a source of power for electronics [1-3]. In analogy to the basic concept that a spatial periodic arrangement of atoms or molecules constructs a normal crystal, it has been investigated that a photonic crystal can be formed by changing the relative permittivity of a material with an appropriately repeating pattern in space.

Since a photonic crystal possesses a forbidden frequency band, called a photonic band-gap, in which propagation of electromagnetic waves is prohibited, the light-reflection principle in the photonic crystal structure can produce many of the analogous optical phenomena, such as spontaneous emission control, strong localization of photons, and low-loss wave-guiding, akin to the atomic potential acting on electrons [4-6]. Thereby, electromagnetic waves are effectively controlled either to propagate through the structure or not, depending on operating wavelengths.

In this paper, cylindrical photonic crystal waveguides (CPCWs) with high-index cores are first proposed and analyzed by accurate computational methods. Here, the high-index core can be realized by inserting materials with higher refractive index values than normal pure-silica glass, such as carbon dioxide, liquefied petroleum

Received: November 21, 2019
Reviewed: January 24, 2020
Accepted: February 3, 2020
* Corresponding Author

ISSN: 2207-6360 IJAST

gas (LPG), and nitrous oxide, into the CPCW. Two numerical approaches of the rigorous full-vector finite-difference time-domain (FDTD) technique and finite difference method (FDM) are considered for cross-verification purpose. Several important propagation characteristics, such as the normalized propagation constant, chromatic and waveguide dispersion, mode field distribution, and effective area, are investigated.

In terms of communication component applications, the normal photonic crystal waveguide is well renowned because of remarkable single-mode operation over incommensurable bandwidth [7][8]. This advantage can be clearly confirmed for the CPCWs by using the FDTD approach during initial investigation. And effective area controllability by the high refractive index of the core is also considered for computational analyses.

2. ELEMENTARY FUNDAMENTALS FOR THE PROPOSED CPCWS

Cylindrically-varying PCWs have periodic index variations only in the azimuthal direction. These waveguides consist of a central core surrounded by a cladding region composed of several alternating-index rings with one equal-thickness repeating pattern. Here, CPCWs with high-index cores are investigated. These kinds of high-index core waveguides can be realized by manufacturing from well-designed preforms for specific optical components or relevant fundamental concepts can be utilized for sensor applications when the waveguide cores are filled with high-index materials.

2.1. DESIGN OF THE CPCWS WITH HIGH-INDEX CORES

The refractive index profile for the proposed geometries is shown in Fig. 1. These optical guides consist of a solid core with a radius of r_1, and air and silica-glass layers, of which thicknesses are denoted by da and ds in the refractive index profile, respectively. Therefore, the two da and ds layers together form one repeating period.

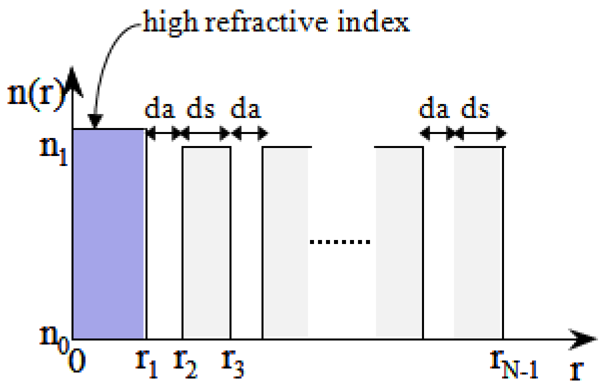

Fig. 1 Refractive index profile of a cylindrically-varying PCW with a high-index core

In Fig.1, the high refractive index (n_c) region can be made of any kinds of gaseous, liquid, or solid materials, which are modelled with index values of 1.45, 1.5, and 1.6 in this investigation. Therefore, the designed optical guides are composed of two or three different materials with uniform cylindrical structures along the wave-propagation axis. Individual sizes for the proposed CPCWs and constituent number of repeat periods can be determined using the following well-reputed calculation approaches.

2.2. ACCURATE COMPUTATIONAL ANALYSIS METHODS

Since the difference between two refractive index values in the periodically-repeating rings of the cladding region can be large, it is necessary to apply a full vectorial approach instead of a scalar-wave approximation to analyze CPCWs. Considering one such light-guiding fiber, which is composed of N linear, isotropic, homogeneous and cylindrically symmetric dielectric layers as illustrated in Fig. 1, the i-th region, which is filled with a refractive index n_i, is defined by an inner radius $r_{(i-1)}$ and an outer radius r_i, where i = 1, 2, · · ·, N. Because of the periodic index profiles, either a high (silica glass) refractive index or a low (air) refractive index is employed for the n_i value. In addition, the core index is designed to be higher than the silica-glass refractive index.

Based on two Maxwell's curl expressions, the proposed CPCWs are investigated by first employing the FDTD method [9]. Considering that the Ex, Ey, Ez, Hx, Hy, and Hz components of electromagnetic fields are inter-related in the rectangular coordinate system, electric and magnetic wave interactions with general three-dimensional objects can be described by six coupled partial differential equations [10].

Furthermore, these six equations are discretized in the space and time domains and used to find field solutions numerically, by assigning a grid point in the rectangular lattice with digitized integers of l, m, n, and v as

$$[l, m, n] = [l\Delta x, m\Delta y, n\Delta z] \tag{1}$$

and any function of space and time as

$$F^{v}(l, m, n) = F(l\Delta x, m\Delta y, n\Delta z, v\Delta t) \tag{2}$$

where Δx, Δy, and Δz are the lattice space increments in the x, y, and z coordinate directions, respectively, and Δt is the time increment [11]. By taking central finite difference approximation for space and time derivatives that are accurate to the second order, the partial derivatives are expressed as

$$\frac{\partial F^{v}(l, m, n)}{\partial x} = \frac{F^{v}\left(l+\frac{1}{2}, m, n\right) - F^{v}\left(l-\frac{1}{2}, m, n\right)}{\Delta x} + O\left(\Delta x^{2}\right) \tag{3}$$

$$\frac{\partial F^{v}(l, m, n)}{\partial t} = \frac{F^{\left(v+\frac{1}{2}\right)}(l, m, n) - F^{\left(v-\frac{1}{2}\right)}(l, m, n)}{\Delta t} + O\left(\Delta t^{2}\right). \tag{4}$$

Along with extending the FDTD logic further in the cross section for the proposed waveguide, infinite electromagnetic media for an arbitrary interesting object need to be modeled carefully. This is because computer memory is not limitless for the computation space, despite the advanced level of current technology. Moreover, in modeling regions extending to infinity, a perfectly matched layer (PML) to make a highly absorbing boundary condition satisfied is effectively implemented at the outer material boundary of a computation domain. Ideally, the absorbing medium is only as thick as a few lattice cells, reflectionless to all impinging electromagnetic fields, highly absorbing, and effective over the full range of operating wavelengths.

There are several parameters to choose for the FDTD computer calculation of the proposed dielectric waveguides, which are approximated by building up computational unit cells for which field component positions are disposed with the desired values of electric permittivity and the normal defined constant of free-space magnetic permeability. Here, the side length of each unit cell is properly chosen to be 0.02 μm for enough accuracy. With an appropriately sized calculation region, 10 PML cells are utilized for perfectly matching to the outer lattice boundary.

The FDTD method is an efficient technique for computation of the normalized propagation constants of guided modes. In order to find the effective refractive index ($\overline{\beta}$) variation, a reasonable axial propagation constant (β) also needs to be chosen, so that the operation wavelength associated with the β value of the fundamental mode can be calculated. By generating the source of an impulse function in the time domain covering an infinite spectrum, the proposed waveguide can be excited. Figure 2 shows spectral data for different β values. Here, Figs. 2(a), 2(b), and 2(c) are analysis results for the CPCW designed with $n_c = n_1 = 1.45$, $r_1 = 1.0$ μm, da = 0.2 μm, ds = 0.3 μm, and a total of 8 layers. Figs. 2(d), 2(e), and 2(f) are for the CPCW designed with $n_c = n_1$, $r_1 = 0.5$ μm, da = 0.2 μm, ds = 0.3 μm, and a total of 8 layers.

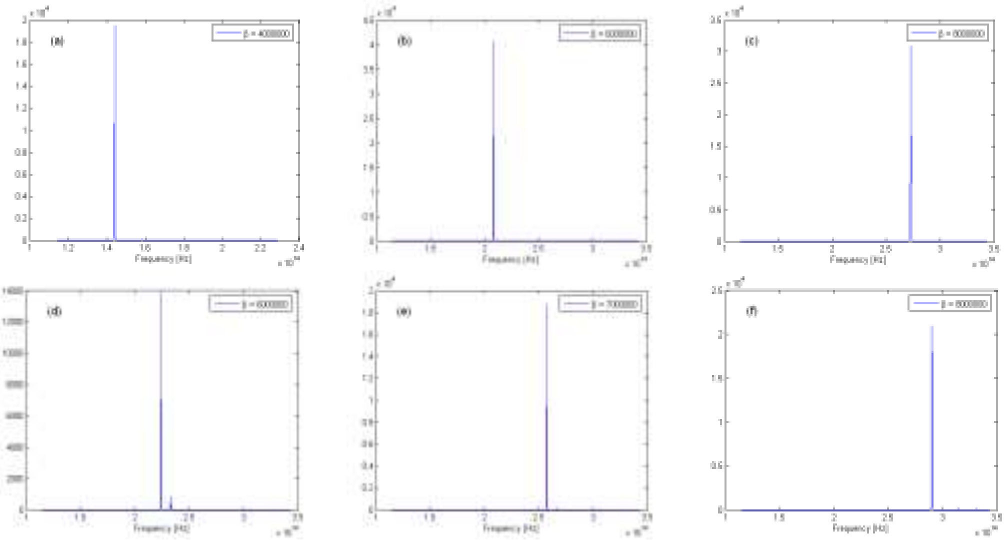

Fig. 2 Spectrum for the fundamental mode of the CPCW designed with $n_c = n_1$, $r_1 = 1.0$ μm, when (a) β = 4000000, (b) β = 6000000, and (c) β = 8000000, and for the CPCW designed with $n_c = n_1$, $r_1 = 0.5$ μm, when (d) β = 6000000, (e) β = 7000000, and (f) β = 8000000

Once spectral data for different β values are provided, mode index results as a function of normalized wavelengths can be computed. For example, when β = 8000000 as in Fig. 2(c), the normalized propagation constant can be found to be about 1.40123 by using the frequency value of 2.726×10^{14} as follows [12]:

$$\overline{\beta} = \frac{\beta}{2\pi}\lambda = \frac{8000000}{2\pi}\,\frac{3.0\times10^{8}}{2.72598\times10^{14}} \approx 1.4012263 \qquad (5)$$

Similar to the FDTD employment, the FDM algorithm is reasonably applied to compute propagation characteristics such as effective refractive index, electromagnetic field profile, and effective mode area [10]. As an initial investigation, complicated structures of the same proposed CPCWs are exploited to yield the normalized propagation constants, which are compared with the results from the FDTD algorithm. Figures 3 and 4 illustrate the normalized propagation constant versus the operation wavelength (λ) for the fundamental mode without taking into account the material dispersion effect [12].

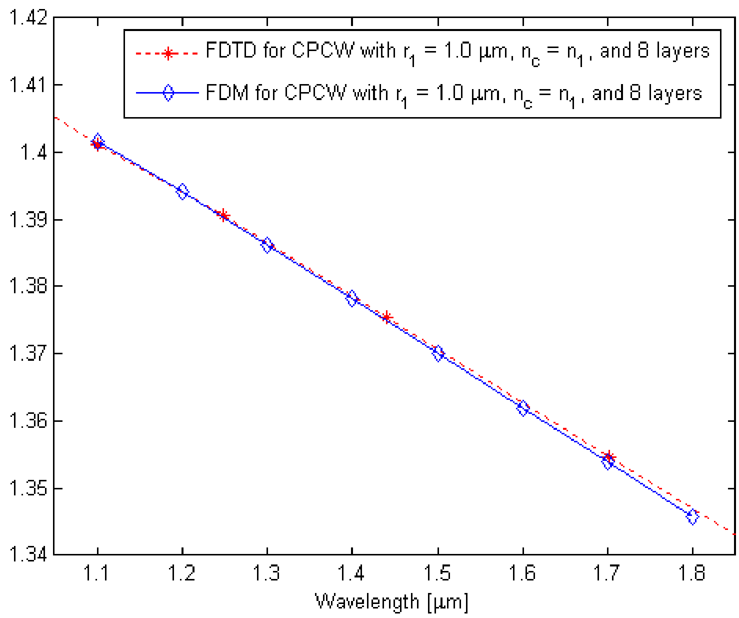

Fig. 3 Variations of the normalized propagation constant versus the operation wavelength for the CPCW with $n_c = n_1$, r_1 = 1.0 μm, da = 0.2 μm, ds = 0.3 μm, and a total of 8 layers

As clearly noticed in Fig.3 for the CPCW designed with $n_c = n_1$ = 1.45, r_1 = 1.0 μm, da = 0.2 μm, ds = 0.3 μm, and a total of 8 layers, results from FDTD and FDM, which are denoted by the dashed line with the star symbol and the solid line with the diamond symbol, respectively, agree very well. The difference is almost negligible. Also, it is reasonably observed that, since one sharp spike exists in each spectrum in Fig. 2(a) for β = 4000000, Fig. 2(b) for β = 6000000, and Fig. 2(c) for β = 8000000, there is strong single-mode operation through the operation wavelength from 1.1 to 1.8 μm, which is remarkably optimistic for realistic communication applications.

Again for the CPCW designed with $n_c = n_1$ = 1.45, r_1 = 0.5 μm, da = 0.2 μm, ds = 0.3 μm, and a total of 8 layers, it is noticed that the normalized propagation constant results from FDTD and FDM, which are denoted by the dashed curve with the star symbol and the solid curve with the diamond symbol, respectively, also agree well as in Fig. 4. Here, based on the strongest sharp pick in each spectrum in Fig. 2(d) for β = 6000000, Fig. 2(e) for β = 7000000, and Fig. 2(f) for β = 8000000, the effective refractive indices are computed to be about 1.2798, 1.2992, and 1.3172 at the operating wavelengths of 1.3402, 1.1661, and 1.0345, respectively.

While the elementary fundamental evaluation tools, based on FDTD and FDM algorithms, are cross-verified, the overall operation tendency can be analyzed computationally. The present detailed verification provides a solid and reliable basis for further investigation in this research as well.

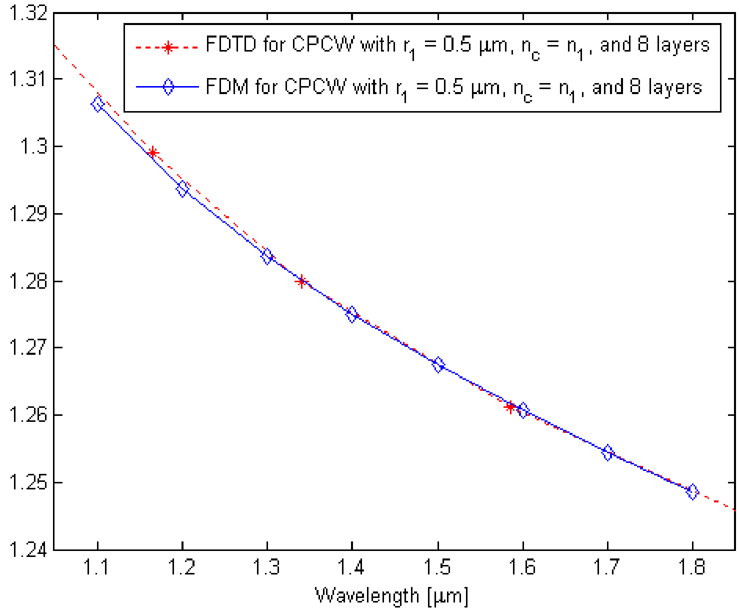

Fig. 4 Variations of the normalized propagation constant versus the operation wavelength for the CPCW with $n_c = n_1$, $r_1 = 0.5$ μm, da = 0.2 μm, ds = 0.3 μm, and a total of 8 layers

In particular, by extensively utilizing the FDM technique, the effective core area variations among the several electromagnetic characteristics are explored in the following section. Thus, evaluation of how moderately effective area values can be controlled is carried out for the proposed CPCWs and electromagnetic results are compared with the previous research achievements [13].

3. ELECTROMAGNETIC PROPAGATION CHARACTERISTICS

In pursuit of more extensive investigation on the effect of the high refractive index of the core, the CPCWs with $n_1 = 1.45$, $r_1 = 0.5$ μm, da = 0.2 μm, ds = 0.3 μm, and a total of 8 layers are designed and analyzed by varying the n_c value to be 1.45, 1.5, and 1.6. Figure 5 depicts the normalized propagation constant versus the operation wavelength for the fundamental mode without taking into account the material dispersion effect [12]. It is noticed that the effective refractive indices for the CPCWs with n_c=n_1 and n_c=1.5 are about 1.284 and 1.312, respectively, which indicates that the normalized propagation constant is changed by 0.028 at $\lambda = 1.3$ μm, while the n_c value is by 0.05. By the way, when the n_c value is changed by 0.1 from 1.5 to 1.6 and the normalized propagation constant is by 0.08 from 1.312 to 1.392. Therefore, the n_c value is changed double from 0.05 to 0.1, meanwhile the normalized propagation constant is more drastically changed by about 2.86 times.

In continuing the exploit by comparative investigation, the CPCWs with $n_1 = 1.45$, $r_1 = 1.0$ μm, da = 0.2 μm, ds = 0.3 μm, and a total of 8 layers are also designed and analyzed by varying the n_c value of the core to be 1.45, 1.5, and 1.6. Figure 6 shows the effective refractive index versus the operating λ for the fundamental mode. Now it is noticed that the effective index values vary almost linearly and inversely proportional to the wavelength. And the CPCW with $r_1 = 1.0$ μm and n_c =1.6 provides much higher effective index values than 1.55 around $\lambda = 1.1$ μm.

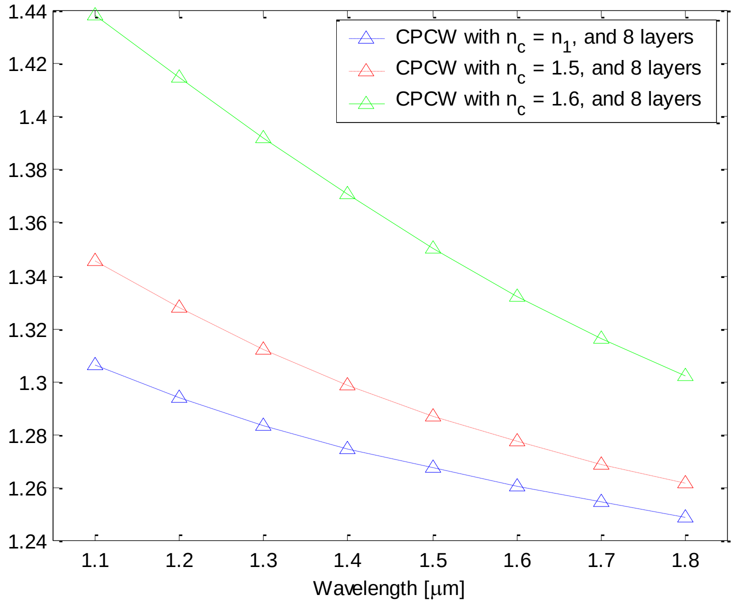

Fig. 5 Variations of the effective refractive index versus the operation wavelength from 1.1 to 1.8 μm for the CPCWs with r_1 = 0.5 μm

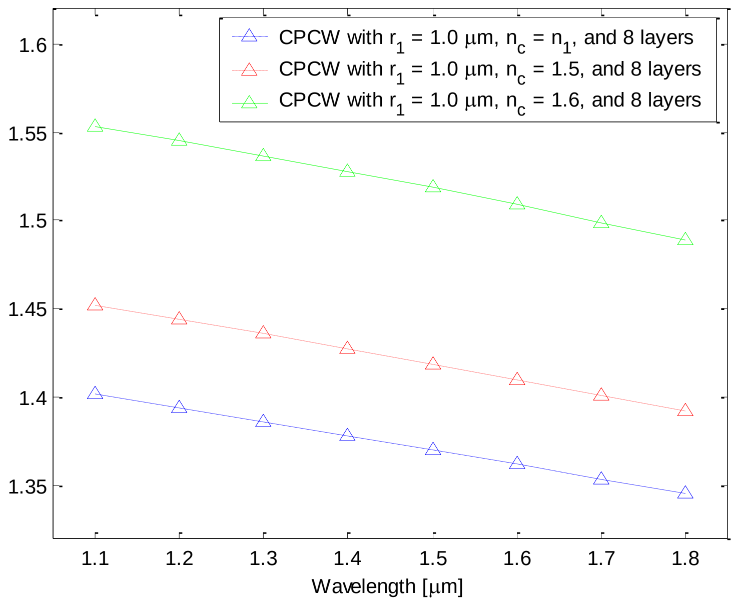

Fig. 6 Variations of the effective refractive index versus the operation wavelength from 1.1 to 1.8 μm for the CPCWs with r_1 = 1.0 μm

During the investigation, electromagnetic field variations are also analyzed. Figure 7 shows field distributions for the Ex electric components of the fundamental mode at the operation wavelength of 1.3 μm by the difference of $n_c=n_1$ and n_c=1.6 for the CPCW designed with r_1 = 0.5 μm, da = 0.2 μm, ds = 0.3 μm, and a total of 8 layers. As expected, more significant discontinuities are noticed at dielectric boundaries for the CPCW with $n_c=n_1$, compared to the CPCW with n_c=1.6, which means electromagnetic energy is more tightly confined for the CPCW design with n_c=1.6.

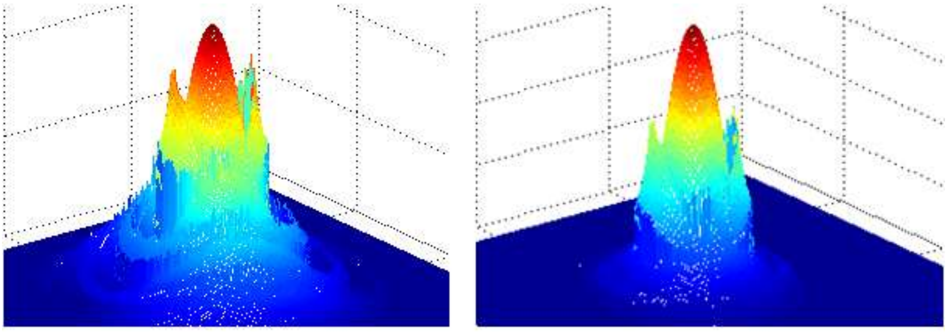

Fig. 7 Ex electric field distributions of the fundamental mode at the operating λ = 1.3 μm for the CPCW designed with (a) n_c=n_1 and (b) n_c=1.6

For nonlinear optical component applications, a smaller effective mode area generally amounts to better nonlinearity, because the nonlinearity is inversely proportional to the effective area of the fundamental mode [14]. Figure 8 plots variations of the effective core area, which are represented by the blue dashed curve, the red dotted curve, and the green solid curve with the up-triangle symbols for the CPCW with r_1 = 0.5 μm, da = 0.2 μm, ds = 0.3 μm, and a total of 8 layers when n_c = n_1, n_c = 1.5, and n_c = 1.6, respectively.

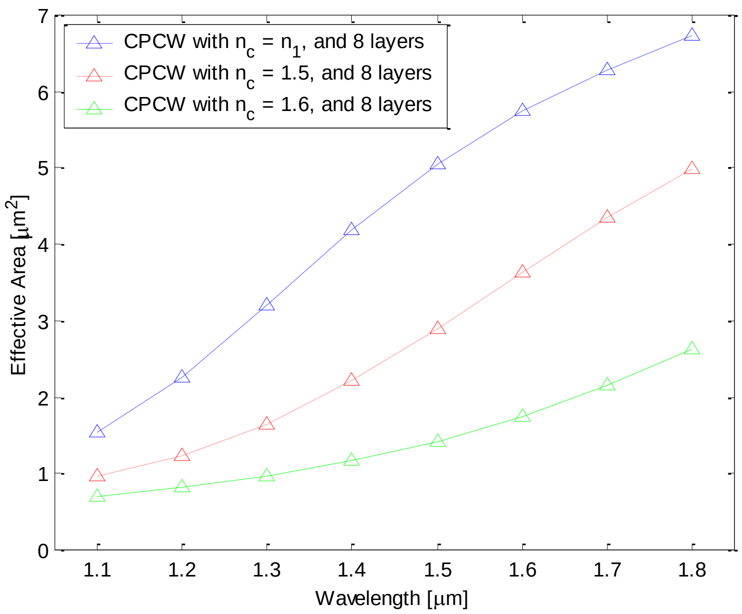

Fig. 8 Variations of the effective mode area versus the operation wavelength for the CPCWs with r_1 = 0.5 μm

Since the mode fields spread more rapidly with longer operating wavelengths, it is well observed that the effective mode areas also become larger. In addition, when the core refractive index is higher as shown in Fig. 7 for the CPCW design with n_c=1.6, the effective area results are generally smaller, compared to the results for the CPCW design with $n_c=n_1$. Figure 9 shows variations of the effective area, which are denoted by the blue dashed, the red dotted, and the green solid curves with the up-triangle symbols for the CPCW with r_1 = 1.0 μm, da = 0.2 μm, ds = 0.3 μm, and a total of 8 layers when $n_c = n_1$, n_c = 1.5, and n_c = 1.6, respectively. Here it is noticed that the effective mode areas change more drastically over the longer operation wavelengths. Meanwhile, the effective areas result in very small values, specifically 0.9615×10^{-12} m^2 and 1.9632×10^{-12} m^2 when r_1 = 0.5 μm and r_1 = 1.0 μm, respectively, at the operating λ = 1.3 μm for the CPCW designed with n_c = 1.6, n_1 = 1.45, da = 0.2 μm, ds = 0.3 μm, and a total of 8 layers. This result reasonably indicates that the proposed CPCW is also optimistic for optical nonlinear applications.

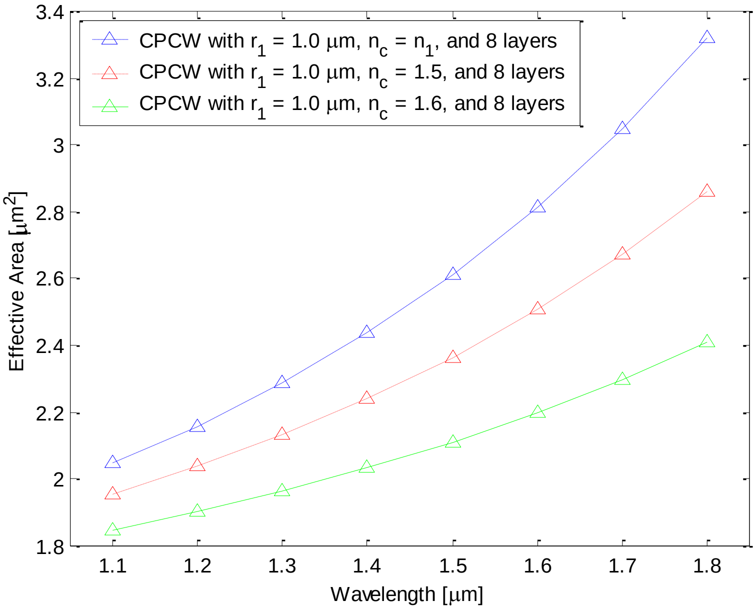

Fig. 9 Variations of the effective mode area versus the operation wavelength for the CPCWs with r_1 = 1.0 μm

4. CONCLUSIONS

CPCWs with high-index cores are first designed and analyzed for accurate full-vector electromagnetic investigation. The high-index core can be realized by inserting materials with higher refractive index values than normal pure-silica glass, such as carbon dioxide, LPG, and nitrous oxide, into the CPCW. Firstly, in order to see the normalized propagation constant dependency on the core refractive index variation, the material dispersion effect is not taken into account. It is reasonable that more significant discontinuities are noticed at dielectric boundaries for the CPCW with $n_c=n_1$ at the operating λ = 1.3 μm, compared to the CPCW with n_c=1.6 and a total of 8 layers, which means electromagnetic energy for the fundamental mode is more tightly confined for the CPCW designed with n_c=1.6 and the same number of layers. Based on the accurate computational analysis, the proposed CPCW provides the strong single-mode operation over the operation wavelength from 1.1 to 1.8 μm, which is remarkably optimistic for realistic communication applications.

With respect to the normalized propagation constant variations, the result for the CPCW with n_c=1.6 indicates more rapid change, compared to the CPCW with the lower core index, when increasing the operation wavelengths from 1.1 μm to 1.8 μm. The effective mode areas result in very small values, specifically 0.9615×10^{-12}

m^2 and 1.9632×10^{-12} m^2 when r_1 = 0.5 μm and r_1 = 1.0 μm, respectively, at the operating λ = 1.3 μm for the CPCW designed with n_c = 1.6, n_1 = 1.45, da = 0.2 μm, ds = 0.3 μm, and a total of 8 layers. By utilizing the propagation characteristics, such as the normalized constant dependency and electromagnetic field variations, inventive applications for optical sensors and nonlinear optical components can be expected to be desirably designed, constructed, and exploited.

REFERENCES

[1] A. A. Rifat, K. Ahmed, S. Asaduzzaman, B. K. Paul, and R. Ahmed. Development of Photonic Crystal Fiber-Based Gas/Chemical Sensors, Computational Photonic Sensors. Switzerland: Springer Nature, (2019).

[2] Md. S. Islam, J. Sultana, A. Dinovitser, K. Ahmed, B. W.-H. Ng, and D. Abbott. "Sensing of Toxic Chemicals Using Polarized Photonic Crystal Fiber in the Terahertz Regime." Optics Communications 426 (2018): 341-347.

[3] D.-K. Hwang, B. Lee, and D.-H. Kim. "Efficiency Enhancement in Solid Dye-Sensitized Solar Cell by Three-Dimensional Photonic Crystal." RSC Advances 3.9 (2013): 3017-3023.

[4] E. Yablonovitch. "Inhibited Spontaneous Emission in Solid-State Physics and Electronics." Physical Review Letters 58.20 (1987): 2059-2062.

[5] S. John. "Strong Localization of Photons in Certain Disordered Dielectric Superlattices." Physical Review Letters 58.23 (1987): 2486-2489.

[6] J. I. Kim. "Investigation of Cladding Effects on Optical Guidance of Microstructured Holey Fibres Based on FDM and FDTD Methods." Journal of Modern Optics 56.9 (2009): 1091-1095.

[7] J. Kim. "Study on Electromagnetic Wave Propagation Characteristics in Cylindrical Photonic Crystal Waveguides with High-Index Cores." 2019 1st Domestic and International Integration Conference, Jeju, Korea, 18-20 August 2019. International Journal of Energy, Information and Communications, (2019), Vol. 10. pp. 1-6.

[8] C.-G. Wang, L. Wang, X. She, N. Li, K. Chen, and X.-W. Shu. "Filament Fusion of Hollow-Core Photonic Crystal Fiber and Single Mode Fiber: Numerical Simulation and Experimental Analysis." Laser Physics 29.5 (2019): 055102.

[9] A. Taflove and S. C. Hagness. Computational Electrodynamics: the Finite-Difference Time-Domain Method. Boston: Artech House, (2005).

[10] J. Kim. “Effects of Core and Cladding on Optical Guidance Properties of Holey Fibers”. Optical Communication, InTech, (2012), pp. 25-40.

[11] K. S. Kunz and R. J. Luebbers. The Finite Difference Time Domain Method for Electromagnetics. CRC Press: Boca Raton, (1993).

[12] G. Keiser. Optical Fiber Communications. New York: McGraw Hill, (2000).

[13] J. Kim. "Effective Area Control by Tailoring the Central Core Hole in Air-Core Cylindrical Photonic Crystal Waveguides." International Journal of Advanced Science and Technology 127 (2019): 41-50.

[14] G. P. Agrawal. Nonlinear Fiber Optics. San Diego: Academic Press, (2001).

